Synthesis of Polyaniline/MCM-41 Composite through Surface Polymerization of Aniline

Xiaomiao Feng, Gang Yang, Yuge Liu, Wenhua Hou, Jun-Jie Zhu

Key Laboratory of Mesoscopic Chemistry and Key Laboratory of Analytical Chemistry for Life Science, School of Chemistry and Chemical Engineering, Nanjing University, Nanjing 210093, China

Received 22 September 2005; accepted 15 November 2005
DOI 10.1002/app.23836
Published online in Wiley InterScience (www.interscience.wiley.com).

ABSTRACT: Polyaniline (PANI)/porous silica MCM-41 (MCM-41) composite was synthesized according to surface polymerization theory, and it was confirmed through comparing with PANI/solid silica (SiO_2) by TGA and XPS techniques. The morphology and composition of the composite were also characterized by some techniques such as small-angle XRD, N_2-adsorption isotherm, SEM, FTIR, and UV–vis. The thermal stability for the PANI/MCM-41 composite was enhanced when compared with that of pure PANI. With the increase in the concentration of HCl, the doping degree increased and UV-absorption peak at about 700 nm showed a red shift. The conductivity of the composite was enhanced by increasing the concentration of HCl. The results of FTIR showed that there was a strong interaction between PANI and MCM-41. © 2006 Wiley Periodicals, Inc. J Appl Polym Sci 101: 2088–2094, 2006

Key words: polyaniline; MCM-41; surface polymerization; conductive; composite

INTRODUCTION

Polyaniline (PANI), one of most important conducting polymers, has attracted considerable interest because of its advantages such as easy synthesis and good environmental ability as well as its electronic, biological, and optical properties.[1–4] However, PANI is insoluble in common solvents and not molten in nature, which limits its applications. To compensate the defects, PANI should be modified by incorporation of inorganic materials. Because PANI/inorganic nanocomposites combine the merits of PANI and inorganic nanoparticles, extensive research has been carried out in this field.[5] Various inorganic materials for the development of the PANI/inorganic composites have been reported.[6–11]

Among those inorganic materials, silica nanoparticles have received great attention because of their unique properties and wide applications.[12] Primarily, the objective of the research is to keep the conducting polymer in a stable colloidal form, and this was pioneered by Armes et al.[13] They succeeded in incorporating big silica particles (~1 μm) into the core of PANI. Aniline was polymerized by ammonium persulfate in the presence of silica colloids at low concentration of monomer and oxidant. The purpose of this technique is to slow down the rate and degree of polymerization and promote the polymerization on the colloidal surface rather than in bulk. Effectively, the outer PANI layer of PANI/SiO_2 colloids is soluble to some extent. Repeat experiment was preformed by using ultrafine colloidal silica (diameter less than 40 nm).[14,15] The high-resolution TEM images confirmed that the PANI/SiO_2 composite had an unusual "raspberry" morphology. These dispersions had good long-term colloidal stability. Wang[16] prepared the PANI/SiO_2 hybrids by using sol–gel process. The resultant hybrids had a good dispersibility and self-assembly of the conductive PANI network in the inorganic network. The electrical conductivity of the hybrids with 20 wt % silica was four times higher than that of the pure PANI. The PANI/SiO_2 composite conductive capsules and hollow spheres had recently been prepared by using monodispersed polystyrene particles as template.[17] The resultant samples were self-stabilized and doped *in situ* without external additives. By incorporating silica into PANI host shell, the hybrid capsules and hollow spheres became strong while keeping the same conductivity level. Porous silica possesses high surface area, and the size of pores can be tuned from 2 to 10 nm in a narrow diameter distribution by changing the experimental conditions. Depending on the channel arrangement, the mesoporous silica is further divided into hexagonal mobile composition of matter (MCM)-41, cubic MCM-48, and lamellar MCM-50.[18] Synthesis of PANI in the porous silica channels has attracted more and more attention. Wu

Correspondence to: J. J. Zhu (jjzhu@nju.edu.cn.) and W. H. Hou (whou@nju.edu.cn).

Contract grant sponsor: National Natural Science Foundation of China; contract grant number: 20325516.

and Bein[19] fabricated a conductive filament of PANI in MCM-41 by using MCM-41 host that was contacted with aniline gas at 313 K for 24 h, which showed significant conductivity. Cho et al.[20] also synthesized the PANI/MCM-41 composite using the same method with that of Wu. This composite shows the property of electrorheology more than that of MCM-41 or PANI alone as a result of the anisotropic polarization of the PANI/MCM-41 composite. PANI/SBA-15 composite was also reported.[21] The impedance of the composite is found to be sensitive to humidity. The range of the variation of the impedance for PANI/SBA-15 is obviously higher than that of bulk PANI. However, both the above composites are prepared by using aniline gas, which is not beneficial to the environment.

Some methods for the preparation of PANI/silica composites such as sol–gel process,[16] ultrasonic irradiation,[22] graft polymerization of aniline,[12] and template method[17] were reported. Surface polymerization is another powerful method for fabricating the PANI/inorganic composite. The polymerization of aniline at the available surface precedes the precipitation polymerization in the bulk.[23–25]

In the present study, we synthesized PANI/MCM-41 composite by using the surface polymerization method. The morphology and composition of the resultant composite were characterized by SEM, FTIR, UV, TGA, XPS. Small-angle XRD and N_2-adsorption isotherms were used to demonstrate that the polymerization of aniline took place not only on the surface but also in the pores of MCM-41. In addition, we investigated the effect of different concentrations of HCl-doped PANI on the optical and electrical properties of PANI/MCM-41 composite.

EXPERIMENTAL

Materials

Aniline, ammonium persulfate (APS), tetraethylsiloxane, and cyltrimethylammonium bromide were purchased from Shanghai Chemical Reagent Co. (Shanghai, China). Aniline was distilled under reduced pressure, and other reagents were used as received without further purification.

Synthesis of PANI/MCM-41 composite

Preparation of MCM-41 was performed according to Ref. 26. The PANI/MCM-41 composites doped with different concentrations of HCl were synthesized by surface polymerization of aniline. For example, PANI/MCM-41 doped with 1*M* HCl was synthesized as follows: 0.1 mL of aniline was mixed with 20 mL of 1*M* HCl under vigorous stirring at room temperature for 30 min. About 0.2 g of MCM-41 was added to the above solution, and the solution was kept vigorous stirring for 30 min to obtain a uniform suspension containing MCM-41. Finally, 5 mL of 1*M* HCl aqueous solution of APS was introduced into the above mixture, and the resulting mixture was allowed to react under gentle stirring for 12 h. The PANI/MCM-41 precipitate was centrifuged and washed with distilled water and ethanol till the filtrate became colorless and then dried at 40°C for 24 h. In the experiment, the molar ratio of aniline to APS was retained at 1:1. PANI/MCM-41 composites doped with other concentrations of HCl (10^{-1}, 10^{-2}, 10^{-3}, 10^{-4}, and $10^{-5}M$) were synthesized using a similar method. Meanwhile, PANI/MCM-41 composites doped with 1*M* of HCl were also synthesized by using different amounts of aniline (0.05, 0.1, and 0.2 mL) for a comparative study.

Furthermore, solid silica (SiO_2) nanospheres with the size of about 150 nm were fabricated as described by Stöber et al.[27] The PANI/SiO_2 composites doped with different concentrations of HCl were synthesized by a similar method as that of PANI/MCM-41. Meanwhile, HCl-doped homo-PANI particles for the comparison were also synthesized by using the conventional oxidation polymerization of aniline. A solution of aniline (0.1 mL) monomer in 1*M* HCl (20 mL) was stirred at room temperature for 30 min. About 5 mL of 1*M* HCl aqueous solution of APS was added to the above solution, and the reaction was maintained for additional 12 h. The molar ratio of aniline to APS is 1:1. The resulting PANI precipitate was washed with a large amount of distilled water. Finally, the product was dried at 40°C for 24 h.

Characterization

FTIR measurements of the samples were performed on Bruker Fourier transform spectrometer model VECTOR 22 using KBr pressed discs. UV–vis spectra were measured on a UV-2401PC UV–vis recording spectrophotometer. The composites were dispersed in distilled water through ultrasound irradiation. Powder X-ray diffraction (XRD) data were recorded using a Shimadzu XD-3A diffractometer with Cu Kα radiation (λ = 0.15418 nm). The morphologies of the products were measured using a JSM-5610LV scanning electron microscope (SEM). Before SEM measurement, the samples were sputtered with thin layers of platinum. X-ray photoelectron spectroscopy (XPS) analysis was carried out using ESCALAB MK II X-ray photoelectron spectroscope. The amount of PANI within the composites was determined using Shimadzu TGA-50 instrument from room temperature to 800°C with a heating rate of 10°C/min in air atmosphere. The conductivities of the samples were measured by a two-probe method using a DT9205 digital multimeter. For each of the conductivities reported, at least three measurements were averaged. N_2-adsorption isotherms were determined at 77 K using nitrogen in a conven-

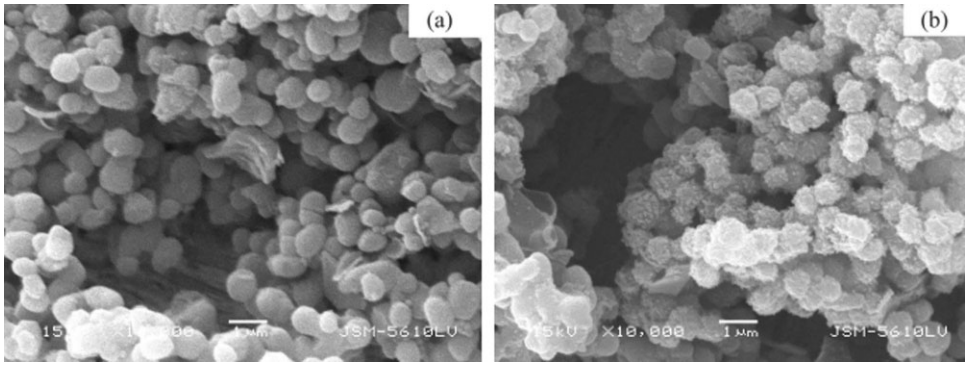

Figure 1 SEM images of (a) MCM-41 and (b) PANI/MCM-41. Synthetic conditions: aniline 0.1 mL, [An]:[APS] = 1:1, MCM-41 0.2 g, [HCl] = 1*M*, reaction time 12 h, reaction temperature 25°C.

tional volumetric technique using a Micromeritics ASAP 2020 surface area and porosity analyzer. Before experiment, the samples were evacuated for 12 h at 120°C. The BET surface area was calculated based on adsorption data in the partial pressure (P/P_0) range 0.01–0.36.

RESULTS AND DISCUSSION

Polymerization of aniline on the surface of MCM-41

The oxidative polymerization of aniline with APS proceeding in aqueous medium has two distinct steps: an induction period, in which the oligomeric species are the main products, followed by the polymerization.[8] In the induction period of aniline polymerization, the oligomeric species mainly exist around the silica and adsorbed by the surface of silica because the polymerization of aniline can be catalyzed by the available surface. The polymerization of aniline has an autocatalytic effect and it is enhanced by the present PANI.[28] Therefore, the aniline polymerization takes place on the surface of silica preceding in the bulk, which results in the formation of PANI-coated silica composite. If the theory of surface polymerization of aniline is correct, the rate of aniline conversion to PANI should be higher in the PANI/MCM-41 system than that of PANI/SiO_2 because the BET surface area is much larger than that of SiO_2.[28] According to the surface polymerization theory, Stejskal and coworkers[28,29] hypothesized that the polymerization of aniline could be catalyzed by the adsorption of an oligomeric intermediate at the available surface, and further, they tested that the surface of silica had a catalytic effect on the initiation of aniline polymerization. Porous silica with different BET surface area was used to test this hypothesis. In their experiment, the external surface area of the particles rather than the total surface area afforded by the pores had a key effect on the catalysis of the reaction. The pores of silica have less effect on the polymerization of aniline because the aniline inside the pores is less accessible to the oxidant. In the present experiment, a gentle stirring was used to make the dispersion of the oxidant in the whole solution. The doping PANI can make all the white MCM-41 particles become green even though the concentration of aniline is very low because the aniline polymerization takes place on the surface of MCM-41 including the pores of MCM-41.

The SEM images of MCM-41 and PANI/MCM-41 are shown in Figure 1. The surface of the pristine MCM-41 is smooth, as shown in Figure 1(a). A characteristic "raspberry" morphology of PANI/MCM-41 is observed in Figure 1(b), because many pores are present on the surface of MCM-41, which lead to the formation of the "raspberry" morphology.

Small-angle XRD patterns of MCM-41 and PANI/MCM-41 are shown in Figure 2. An intense (100) peak,

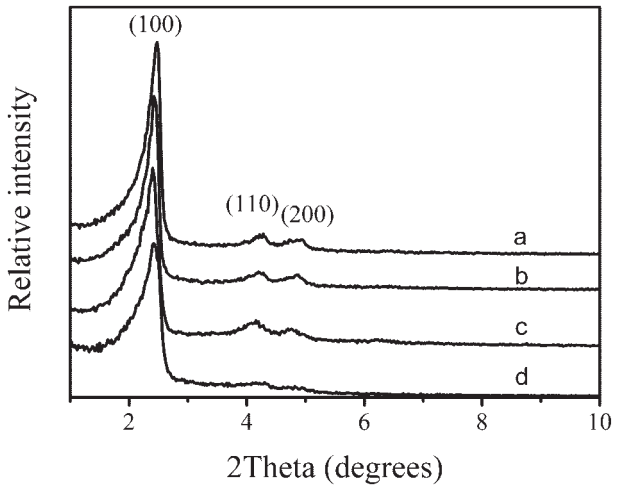

Figure 2 Small-angle XRD patterns of (a) pristine MCM-41 and PANI/MCM-41 synthesized with different amounts of aniline: (b) 0.05 mL, (c) 0.1 mL, and (d) 0.2 mL. Synthetic conditions: [An]:[APS] = 1:1, MCM-41 0.2 g, [HCl] = 1*M*, reaction time 12 h, reaction temperature 25°C.

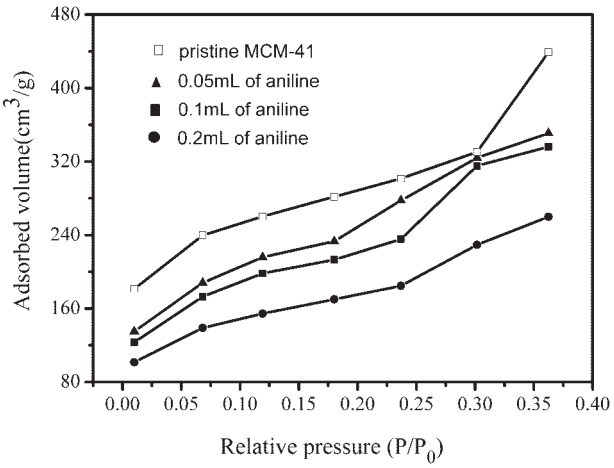

Figure 3 N_2-adsorption isotherm curves of pristine MCM-41 and PANI/MCM-41 prepared with different amounts of aniline. Synthetic conditions: [An]:[APS] = 1:1, MCM-41 0.2 g, [HCl] = 1*M*, reaction time 12 h, reaction temperature 25°C.

followed by minor (110) and (200) peaks, corresponding to a highly ordered hexagonal structure of MCM-41 [Fig. 2(a)] is observed for pristine MCM-41. An obvious reduction in the peak intensities takes place after aniline polymerization as shown in Figures 2(b)–2(d) because of the inclusion of the polymerization of aniline in the channels. Moreover, with the increasing amount of aniline, the decreasing level of the intensity for the (100) peak is more significant. The minor (110) and (200) peaks disappear when the amount of aniline is 0.2 mL.

The PANI confined within the channels of MCM-41 is also confirmed by a nitrogen sorption measurement. The N_2-adsorption isotherm curves of both the pristine MCM-41 and PANI/MCM-41 composites prepared by using different amounts of aniline are represented in Figure 3. The BET surface area of the pristine MCM-41 is 1034.9389 m^2/g. When the amount of aniline is 0.05, 0.1, and 0.2 mL, the BET surface areas of the PANI/MCM-41 composites are 989.2947, 950.9025, and 716.9462 m^2/g, respectively. The decrease in BET surface area and the amount of nitrogen adsorbed volume for PANI/MCM-41 composites in comparison with that of pristine MCM-41 clearly shows that PANI is present in the pores of MCM-41. A similar decrease in specific area is observed after entrapment of poly(diphenylamine)[30] and enzymes.[31]

Structural characterization and confirmation of the theory of surface polymerization

The FTIR absorption spectra of PANI, SiO_2, MCM-41, PANI/MCM-41, and PANI/SiO_2 are shown in Figure 4. In the case of pure PANI, the main peaks at 1563 and 1481 cm^{-1} can be assigned to the stretching vibrations of quinone and benzene rings, respectively. The peaks at 1298 and 1243 cm^{-1} correspond to the C—N stretching vibration. The in-plane bending of C—H is reflected in the 1123 cm^{-1} peak. The peak at 799 cm^{-1} is attributed to the out-of-plane bending of C—H. The Si—O—Si symmetric stretching mode of SiO_2 and MCM-41 occur at 1097 and 1086 cm^{-1}, respectively. Both the peaks at 1096 cm^{-1} for PANI/SiO_2 and at 1083 cm^{-1} for PANI/MCM-41 can be assigned to the overlap of the in-plane bending of C—H and Si—O—Si symmetric stretching vibration. The stretching modes of quinone and benzene rings are located at 1579 and 1492 cm^{-1} versus 1568 and 1487 cm^{-1} for PANI/MCM-41 and PANI/SiO_2, respectively. The C—N stretching vibrations for PANI/MCM-41 and PANI/SiO_2 appear at 1303 and 1245 cm^{-1}, 1301 and 1245 cm^{-1}, respectively. In addition, the IR bands for the out-of-plane bending of C—H are in good agreement with the values of 803 and 801 cm^{-1} for PANI/MCM-41 and PANI/SiO_2, respectively. For the two composites, the absorption peaks of quinone and benzene rings, C—N stretching vibrations and out-of-plane bending of C—H are all shifted to higher wave numbers compared with that of PANI homopolymer. The results show a strong interaction between PANI and silica, which is identical with the results of Ref. 22. The IR data indicates that the C═C, C—N, and C—H bands within the polymer are influenced by the silica particles. The shifts of the adsorption peaks for these groups are directly related to the differences in electron density. Because there are many —OH groups on the surface of silica, the electron density may be changed when they combine with PANI. The induction effect of —OH leads to the shifts to higher wavenumbers of the adsorption peaks for these groups.

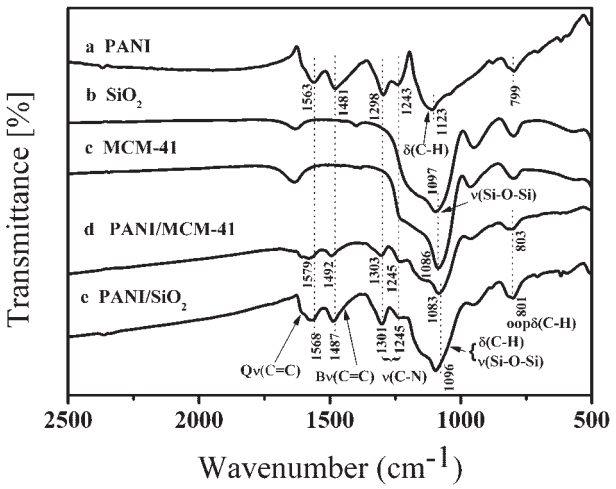

Figure 4 FTIR spectra of (a) PANI, (b) SiO_2, (c) MCM-41, (d) PANI/MCM-41, and (e) PANI/ SiO_2. Synthetic conditions: aniline 0.1 mL, [An]:[APS] = 1:1, SiO_2 (MCM-41) 0.2 g, [HCl] = 1*M*, reaction time 12 h, reaction temperature 25°C.

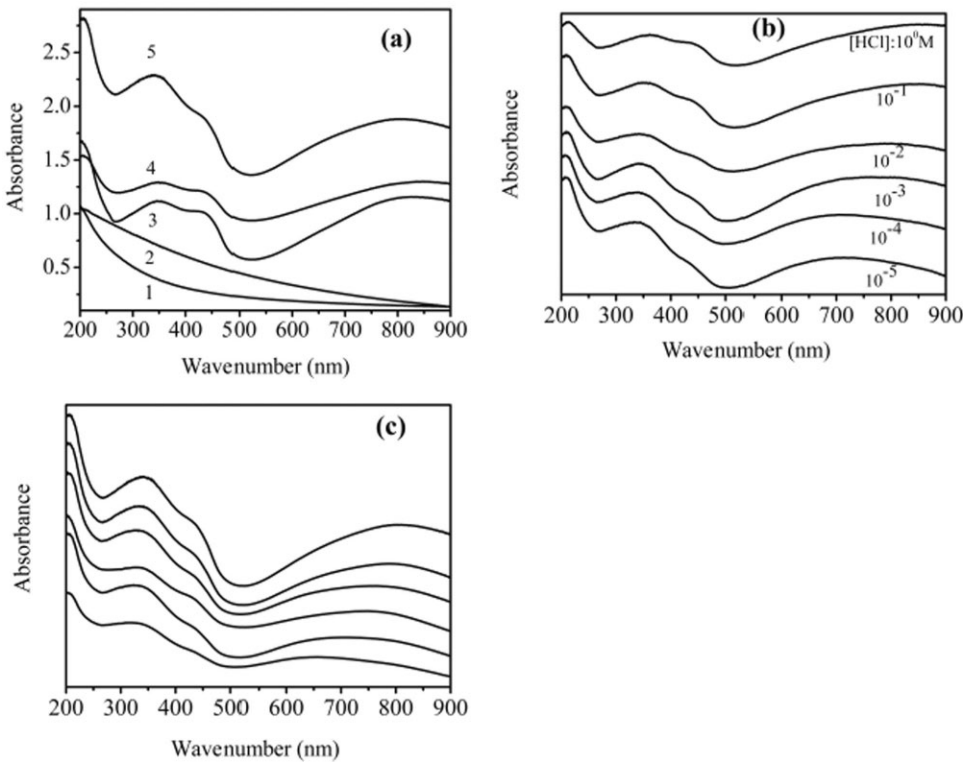

Figure 5 (a) UV–vis absorption spectra of (1) SiO_2, (2) MCM-41, (3) PANI, (4) PANI/SiO_2, and (5) PANI/MCM-41. Synthetic conditions: aniline 0.1 mL, [An]:[APS] = 1:1, SiO_2 (MCM-41) 0.2 g, [HCl] = 1*M*, reaction time 12 h, reaction temperature 25°C. (b) Different concentrations of HCl-doped PANI/SiO_2. (c) Different concentrations of HCl-doped PANI/MCM-41. Concentrations of HCl in (b) and (c) are 10^0, 10^{-1}, 10^{-2}, 10^{-3}, 10^{-4}, and 10^{-5}*M* from high to low, respectively. Other experimental conditions are identical with the former.

The UV–vis spectra of PANI/SiO_2 and PANI/MCM-41 are shown in Figure 5. Figure 5(a) shows that both the composites have similar features as that of pure PANI. They exhibit three characteristic peaks: an absorption peak at ~330–370 nm represents the π–π^* transition of the benzenoid ring,[32] and two absorption peaks at ~430–460 nm and ~700–900 nm can be assigned to the polaron band transitions, while the presence of the peak at ~700–900 nm also proves that the PANI is obtained in doped state. Figures 5(b) and 5(c) show the UV–vis spectra of different concentrations of HCl-doped PANI/SiO_2 and PANI/MCM-41. The absorption peak at about 700 nm shows a red shift to 850 and 825 nm for PANI/SiO_2 and PANI/MCM-41 with the increase in the concentration of HCl from 10^{-5} to 1*M*, respectively. Furthermore, this adsorption peak becomes broader with the increase in the concentration of HCl. This result indicated that the doping degree was higher, and emeraldine salts were more delocalized.[33]

Figure 6 shows the TGA curves of the compositions for pure PANI, PANI/SiO_2, and PANI/MCM-41 composites. The residual weight percentage refers to the weight percentage content of silica in the composite. In general, the thermal behavior of PANI shows a three-step weight loss process, as observed in the three TGA curves indicating the majority weight loss for respective steps. The first weight loss just below 100°C is attributed to the loss of water, and the second weight loss ranging from 200 to 300°C is believed to be

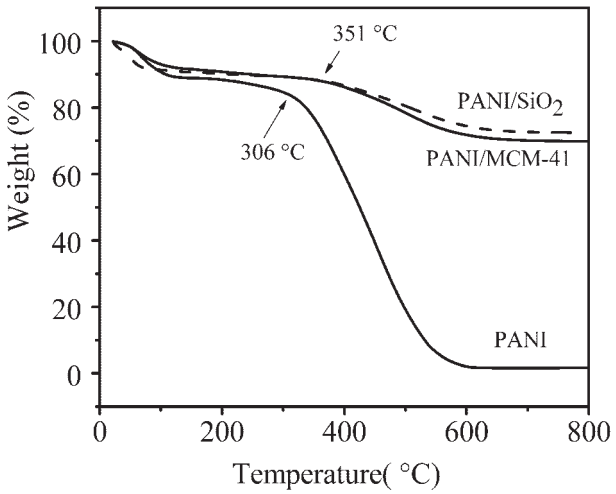

Figure 6 TGA curves of (a) PANI, (b) PANI/SiO_2, and (c) PANI/MCM-41. Synthetic conditions: aniline 0.1 mL, [An]:[APS] = 1:1, SiO_2 (MCM-41) 0.2 g, [HCl] = 1*M*, reaction time 12 h, reaction temperature 25°C.

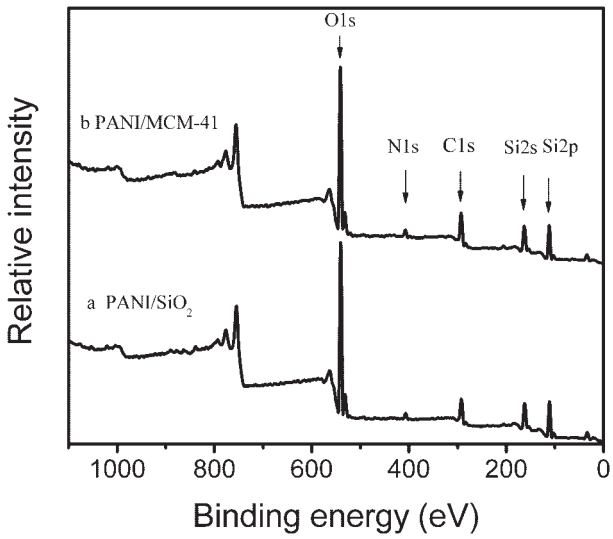

Figure 7 Wide-range X-ray photoelectron spectra of (a) $PANI/SiO_2$ and (b) PANI/MCM-41. Synthetic conditions: aniline 0.1 mL, [An]:[APS] = 1:1, SiO_2 (MCM-41) 0.2 g, [HCl] = 1*M*, reaction time 12 h, reaction temperature 25°C.

due to the departure of acid dopant (HCl).[34] The third weight loss starting at around 306°C is assigned to the decomposition of PANI chains.[35] As a comparison, the third weight loss percentage content of PANI/MCM-41 is about 18.13%, which is higher than that of $PANI/SiO_2$ (15.92%). The result shows that the rate of aniline conversion to PANI in the PANI/MCM-41 composite system is higher than that of $PANI/SiO_2$ composite system in the same experimental conditions, which confirms that the surface has a catalytic effect. Because the specific surface area of the porous silica MCM-41 is much larger than that of solid silica SiO_2, the catalytic effect of the former is stronger than the latter, which results in the higher content of PANI in the PANI/MCM-41 composite. In addition, the temperature of decomposition for PANI chains of the two composites is higher about 45°C than that of pure PANI. Because silica is stable in the range from room temperature to 800°C, when it is combined with PANI, the thermal stability of PANI would be enhanced.

Figure 7 presents the wide scan XPS spectra of $PANI/SiO_2$ and PANI/MCM-41. Table I shows the binding energy and composition of every element in the surface. The binding energy of every element is slightly different owing to the change of environment. The percentage of every atom in the surface of the two composites is determined by the ratios of the peak areas corrected by the empirical sensitivity factors. The Si/N atom ratio on the surface of the $PANI/SiO_2$ is 9.88 and that of PANI/MCM-41 at the same condition is 5.75, which is lower than that of $PANI/SiO_2$. Furthermore, the content of Cl atom is higher in the PANI/MCM-41 composite system than in the $PANI/SiO_2$. The result indicates that the rate of aniline conversion to PANI and doping level of PANI/MCM-41 composite is higher than that of $PANI/SiO_2$ composite, which is consistent with the result of TGA. The theory of surface polymerization of aniline is further confirmed by the results of both TGA and XPS.

TABLE I
Binding Energy of Every Element on the Surface of $PANI/SiO_2$ and PANI/MCM-41

	$PANI/SiO_2$		PANI/MCM-41	
Element	Atomic %	BE (ev)	Atomic %	BE (ev)
C1s	20.51	291.30	23.06	291.95
O1s	54.01	540.45	51.34	540.80
N1s	2.29	405.60	3.65	406.50
Si2p	22.63	110.90	20.99	111.45
Cl2p	0.56	203.25	0.96	203.95

Conductivity

The conductivities of the two composites are shown in Table II. Silica is a kind of insulator, so that when conductive PANI and silica are combined, it forms the conductive channels. The MCM-41 particles are arranged disorderly, and many PANI particles in the pores of MCM-41 hinder the formation of good conductive channels. Although the content of PANI is higher in PANI/MCM-41 than that in $PANI/SiO_2$, the conductivity of PANI/MCM-41 is lower than that of $PANI/SiO_2$. The conductivities of the two composites become higher with the increase in the concentration of HCl.

CONCLUSIONS

PANI/MCM-41 composite was synthesized by chemical oxidative polymerization of aniline on the surface of MCM-41 in the presence of HCl. The result of FTIR suggested a strong interaction between PANI and MCM-41. Small-angle XRD patterns and N_2-adsorption isotherms of PANI/MCM-41 showed that PANI

TABLE II
Conductivities of Different Concentrations of HCl-Doped $PANI/SiO_2$ and PANI/MCM-41

Concentrations of HCl (mol/L)	Conductivity (S/cm)	
	$PANI/SiO_2$	PANI/MCM-41
10^0	3.76×10^{-3}	3.12×10^{-5}
10^{-1}	1.68×10^{-3}	1.71×10^{-5}
10^{-2}	3.79×10^{-4}	1.44×10^{-5}
10^{-3}	3.18×10^{-4}	4.68×10^{-7}
10^{-4}	2.97×10^{-4}	2.48×10^{-7}
10^{-5}	1.31×10^{-4}	1.95×10^{-7}

Synthetic conditions: aniline 0.1 mL, [An]:[APS] = 1:1, SiO_2 (MCM-41) 0.2g, reaction time 12 h, reaction temperature 25°C.

was present not only on the surface of MCM-41 but also in the pores of MCM-41. XPS and TGA indicated that the rate of aniline conversion to PANI in PANI/MCM-41 composite system was higher than that of PANI/SiO_2. These results further confirmed the surface polymerization theory of aniline. Furthermore, TGA measurement confirmed the thermal stability was enhanced after combining with MCM-41. UV–vis spectra indicated that the doping degree was higher and emeraldine salts were more delocalized with the increase in the concentration of HCl. Moreover, with the increase in the concentration of HCl, the conductivity of the composite became higher. The PANI/MCM-41 combined the merits of PANI and silica. The thermal stability of PANI was enhanced by incorporating it into MCM-41, and MCM-41 became conductive after combining with PANI.

References

1. Huang, J. X.; Virji, S.; Weiller, B. H.; Kaner, R. B. J Am Chem Soc 2003, 125, 314.
2. Liu, H.; Hu, X. B.; Wang, J. Y.; Boughton, R. I. Macromolecules 2002, 35, 9414.
3. Tian, S. J.; Liu, J. Y.; Zhu, T.; Knoll, W. Chem Mater 2004, 16, 4103.
4. Riede, A.; Helmstedt, M.; Riede, V.; Zemek, J.; Stejskal, J. Langmuir 2000, 16, 6240.
5. Gangopadhyay, R.; De, A. Chem Mater 2000, 12, 608.
6. Zhang, L. J.; Wan, M. X. J Phys Chem B 2003, 107, 6748.
7. Kinyanjui, J. M.; Hatchett, D. W.; Smith, J. A.; Josowicz, M. Chem Mater 2004, 16, 3390.
8. Sapurina, I.; Fedorova, S.; Stejskal, J. Langmuir 2003, 19, 7413.
9. Wu, Q.; Xue, Z.; Qi, Z.; Wang, F. Polymer 2000, 41, 2029.
10. Chandrakanthi, R. L. N.; Careem, M. A. Thin Solid Films 2002, 417, 51.
11. Ray, S. S.; Biswas, M. Synth Met 2000, 108, 231.
12. Liu, P.; Liu, W. M.; Xue, Q. J. Mater Chem Phys 2004, 87, 109.
13. Armes, S. P.; Gottesfeld, S.; Beery, J. G.; Garzon, F.; Agnew, S. F. Polymer 1991, 32, 2325.
14. Gill, M.; Armes, S. P.; Fairhurst, D.; Emmett, S. N.; Idzorek, G.; Pigott, T. Langmuir 1992, 8, 2178.
15. Stejskal, J.; Kratochvil, P.; Armes, S. P.; Lascelles, S. F.; Riede, A.; Helmstedt, M.; Prokes, J.; Krivka, I. Macromolecules 1996, 29, 6814.
16. Wang, Y. J.; Wang, X. H.; Li, J.; Mo, Z. S.; Zhao, X. J.; Jing, X. B.; Wang, F. Adv Mater (Weinheim, Ger) 2001, 13, 1582.
17. Niu, Z. W.; Yang, Z. Z.; Hu, Z. B.; Lu, Y. F.; Han, C. C. Adv Funct Mater 2003, 13, 949.
18. Cho, M. S.; Choi, H. J.; Kim, K. Y.; Ahn, W.-S. Macromol Rapid Commun 2002, 23, 713.
19. Wu, C.; Bein, T. Science 1994, 264, 1757.
20. Cho, M. S.; Choi, H. J.; Ahn, W.-S. Langmuir 2004, 20, 202.
21. Li, N.; Li, X. T.; Geng, W. C.; Zhang, T.; Zuo, Y.; Qiu, S. L. J Appl Polym Sci 2004, 93, 1597.
22. Xia, H. S.; Wang, Q. J Appl Polym Sci 2003, 87, 1811.
23. Sapurina, I.; Riede, A.; Stejskal, J. Synth Met 2001, 123, 503.
24. Liao, C. P.; Gu, M. Y. Thin Solid Films 2002, 408, 37.
25. Tzou, K.; Gregory, R. V. Synth Met 1992, 47, 267.
26. Cai, Q.; Lin, W. Y.; Xiao, F. S.; Pang, W. Q.; Chen, X. H.; Zou, B. S. Microporous Mesoporous Mater 1999, 32, 1.
27. Stöber, W.; Fink, A.; Bohn, E. J. J Colloid Interface Sci 1968, 26, 62.
28. Fedorova, S.; Stejskal, J. Langmuir 2002, 18, 5630.
29. Stejskal, J.; Trchova, M.; Fedorova, S.; Sapurina, I.; Zemek, J. Langmuir 2003, 19, 3013.
30. Lee, K.-P.; Showkat, A. M.; Gopalan, A. I.; Kim, S.-H.; Choi, S.-H. Macromolecules 2005, 38, 364.
31. Takahashi, H.; Li, B.; Sasaki, T.; Miyazaki, C.; Kajino, T.; Inagaki, S. Chem Mater 2000, 12, 3310.
32. Liu, F. L.; Wudl, F.; Nowak, M.; Heeger, A. J. J Am Chem Soc 1986, 108, 8311.
33. Chen, S. A.; Hwang, G. W. J Am Chem Soc 1995, 117, 10055.
34. Oh, S. Y.; Koh, H. C.; Choi, J. W.; Rhee, H. W.; Kim, H. S. Polym J 1997, 29, 404.
35. Wei, Y.; Hsueh, K. F. J Polym Sci Part A: Polym Chem 1989, 27, 4351.